Chaotic matter shock wave of an open system*

Deng Yan(邓 艳), Hai Wen-Hua(海文华)†,
Rong Shi-Guang(荣识广), and Zhong Hong-Hua(钟宏华)

Department of Physics and Key Laboratory of Low-dimensional Quantum Structures and Quantum Control of Ministry of Education, Hunan Normal University, Changsha 410081*, China*

(Received 30 March 2010; revised manuscript received 3 August 2010)

We investigate a one-dimensional open Bose–Einstein condensate with attractive interaction, by considering the effect of feeding from nonequilibrium thermal cloud and applying the time-periodic inverted-harmonic potential. Using the direct perturbation method and the exact shock wave solution of the stationary Gross–Pitaevskii equation, we obtain the chaotic perturbed solution and the Melnikov chaotic regions. Based on the analytical and the numerical methods, the influence of the feeding strength on the chaotic motion is revealed. It is shown that the chaotic regions could be enlarged by reducing the feeding strength and the increase of feeding strength plays a role in suppressing chaos. In the case of "nonpropagated" shock wave with fixed boundary, the number of condensed atoms increases faster as the feeding strength increases. However, for the free boundary the metastable shock wave with fixed front density oscillates its front position and atomic number aperiodically, and their amplitudes decay with the increase of the feeding strength.

Keywords: Bose–Einstein condensate, feeding strength, shock wave, chaos

PACC: 0530J, 0545, 3690

1. Introduction

Shock wave is a specific nonlinear phenomenon which has been thoroughly investigated in different physical systems[1−4] during the last century. A shock wave in a compressible classical fluid displays a steep jump in gas velocity and density due to the collisions of particles. Recently, it has been found in Bose–Einstein condensates (BECs) consisting of ultracold dilute alkali gases analytically[5−8] and observed experimentally and numerically.[9−11] A one-dimensional (1D) BEC driven by the time-periodic harmonic or/and inverted-harmonic potential[12−18] has been investigated. It is found that the well-known Smale-horseshoe chaos exists in this system when a BEC shock wave is created in a range near the potential centre at an initial time.[12] The exact stationary states and the nonstationary states have been obtained for the case of undriving. The former contains the stable "nonpropagated" shock wave, and in the latter the shock wave alternately collapses and revives for the harmonic trapping or propagates at an exponentially increasing shock-front speed for the antitrapping. It is demonstrated that the existence of chaos plays a role in suppressing the blast of matter wave.[12] However, the above theoretical researches of BEC shock waves have not considered the feeding of the condensate atoms from the nonequilibrium thermal cloud.[19−23] In experiment, it is important to understand how a BEC can be formed from a noncondensed atomic cloud by means of evaporative cooling. By treating the noncondensed cloud as a static "heat bath", the feeding effect practically exists in BEC systems[19] and the feeding can be described by a parameter γ which was estimated to be much less than the trapping frequency.[20] Effects of the feeding on phase transition[21] and chaos[22] have also been investigated. Therefore, for the investigation of the BEC shock waves with taking into account this effect is an interesting topic.

In the present paper, we investigate a 1D open BEC with attractive interaction, which is driven by a time-periodic inverted-harmonic potential. The effect of feeding of the condensate from the nonequilibrium thermal cloud is considered. We find some new and interesting phenomena for such a system due to the feeding effect. In order to research the

*Project supported by the National Natural Science Foundation of China (Grant No. 10875039) and the Construct Program of the National Key Discipline of China (Grant No. 4[2007]), and the Specialized Research Fund for the Doctoral Program of Higher Education, China (Grant No. 200805420002).

†Corresponding author. E-mail: whhai2005@yahoo.com.cn

© 2010 Chinese Physical Society and IOP Publishing Ltd

chaotic properties of the system, by using the direct perturbation method[24−28] and the exact shock wave solution of the stationary Gross–Pitaevskii equation (GPE),[12] we obtain the chaotic perturbed solution for weak driving and small feeding strength. According to the Melnikov-function method[29−32] we give the Melnikov chaotic regions in parameter space. It is revealed that the chaotic regions could be enlarged by inducing the feeding strength. Then we analytically and numerically study the effects of feeding strength on the chaotic motion of the system, and show that the chaos can be suppressed in chaotic regions by increasing feeding strength. The time evolutions of the number of condensed atoms are investigated for different feeding strengths. For a fixed boundary, the "nonpropagated" shock wave increases its number of condensed atoms faster with the feeding strength increasing. However, in the free boundary case, for a kind of metastable shock wave with a fixed front density, the front position and the atomic number oscillate aperiodically. But the oscillation amplitudes decay as the increase of the feeding strength, thereby leading to loss of the metastability. The results suggest a qualitative method of observing the BEC shock waves and of generating and controlling BEC chaos by adjusting the feeding strength experimentally.

2. Chaotic perturbed solution and chaotic regions

The system considered here is a 1D open BEC driven by a time-periodic inverted-harmonic potential with attractive interaction under considering the feeding from the non-equilibrium thermal cloud. The corresponding time-dependent GPE reads

$$\mathrm{i}\hbar\psi_t = -\frac{\hbar^2}{2m}\psi_{xx} + V'(x,t)\psi + g'_{1\mathrm{d}}|\psi|^2\psi + \mathrm{i}\gamma\psi, \quad (1)$$

where m is the atomic mass and $V'(x,t) = (-m\omega_x^2/2 + V'_1\cos\omega t)x^2$ is the inverted-harmonic potential of frequency ω_x with driving strength V'_1 and frequency ω, $0 < \gamma \ll \hbar\omega_x$ is a small parameter related to the feeding of the condensate from the nonequilibrium thermal cloud,[20] and $g'_{1\mathrm{d}} = m\omega_r g_0/(2\pi\hbar) = 2\hbar\omega_r a_\mathrm{s}$ is the quasi-1D atom–atom interaction intensity with $a_\mathrm{s} < 0$ being the s-wave scattering length and ω_r the frequency of transverse harmonic oscillator. Taking an experimentally suitable frequency ω_0 as the units of frequencies ω_x, ω, and normalizing the time, space, and wave function with ω_0^{-1}, $l_0 = \sqrt{\hbar/(m\omega_0)}$ and $1/\sqrt{l_0}$, equation (1) becomes the dimensionless equation

$$\begin{aligned} \mathrm{i}\psi_t &= -\frac{1}{2}\psi_{xx} + k(t)x^2\psi + g_{1\mathrm{d}}|\psi|^2\psi + \mathrm{i}\gamma\psi, \\ k(t) &= -\frac{1}{2}\omega_x^2 + V_1\cos\omega t. \end{aligned} \quad (2)$$

Here, the interaction is reduced to $g_{1\mathrm{d}} = 2\omega_r a_\mathrm{s}/(\omega_0 l_0)$. The driving strength V_1 and the feeding strength γ are normalized by $m\omega_0^2$ and $\hbar\omega_0$, respectively. Throughout the paper we take $g_{1\mathrm{d}} = -0.375$ as an example and let γ be in the small range $0 \le \gamma \le 0.2$.

By transforming $x \to -x$ we notice that equation (2) describes a symmetric BEC system. Therefore we can consider a real physical process in which a BEC is created experimentally between positions $\pm x_0(t_0) = \pm L$ at initial time t_0. Then the condensed atoms propagate along the $\pm x$ directions, and the boundary coordinates $\pm x_0(t)$ are time-dependent. The initial wave function reads[12] $\psi(x,t_0) = F(x)$ for $|x| \le L$, and $\psi(x,t_0) = 0$ for $|x| > L$. For a practical BEC the boundary density $|\psi(\pm L,t_0)|^2 = F^2(L)$ could be made nonzero by using Feshbach resonances,[11] leading to the steep jumps in atomic density and flow velocity, which characterize the features of shock wave.[33] The initial data of $\psi(\pm L,t_0)$ and $\psi_x(\pm L,t_0)$ cannot be measured accurately, but they correspond to a unique solution of Eq. (2) strictly. Therefore if we can construct an exact solution $\psi(x,t)$ to obey the initial wave function, it describes the exact shock wave of the system.

We now take the formally exact solution of Eq. (2) as[12]

$$\psi(x,t) = [A(t)x + \mathrm{i}B(t)]\,\mathrm{e}^{\mathrm{i}[a(t)+b(t)x^2]}, \quad (3)$$

where $A(t)$, $B(t)$, $a(t)$ and $b(t)$ are functions of time. By inserting Eq. (3) into Eq. (2), we easily obtain the coupled equations

$$\begin{aligned} &\dot{A} + 3bA - \gamma A = 0, \\ &\dot{b} + 2b^2 + k(t) + g_{1\mathrm{d}}A^2 = 0, \\ &\dot{a} + g_{1\mathrm{d}}B^2 = 0, \\ &\dot{B} + bB - B\gamma = 0. \end{aligned} \quad (4)$$

Rewriting the wave function Eq. (3) in the exponential form $\psi(x,t) = \sqrt{\rho}\,\mathrm{e}^{\mathrm{i}\theta}$, we have the atomic density and flow velocity

$$\begin{aligned} \rho(x,t) &= |\psi(x,t)|^2 = A^2x^2 + B^2, \\ v(x,t) &= \frac{\hbar}{m}\theta_x = \frac{\hbar}{m}\left(2bx - \frac{AB}{\rho}\right). \end{aligned} \quad (5)$$

From the first formula of Eq. (4) we obtain $b = \gamma/3 - \dot{A}/(3A)$ and $\dot{b} = \dot{A}^2/(3A^2) - \ddot{A}/(3A)$. Applying b and $\dot{b}$ to the second formula of Eq. (4), we arrive at the decoupled equation

$$\ddot{A} = \frac{5\dot{A}^2}{3A} + 3A^3 g_{1\mathrm{d}} + 3Ak(t) + \frac{2}{3}\gamma^2 A - \frac{4}{3}\gamma\dot{A}. \quad (6)$$

It is difficult to find the exact solution of Eq. (6). However, for the case of the weak driving strength and the small feeding strength, we can treat them as perturbations to the system and seek its approximate solution. Expanding A in the first order approximation

$$A = A_0 + A_1, \quad |A_1| \ll |A_0| \quad (7)$$

and inserting it into Eq. (6), we obtain the leading and the first order equations as follows:

$$\begin{aligned}
\ddot{A}_0 &= \frac{5\dot{A}_0^2}{3A_0} + 3A_0^3 g_{1\mathrm{d}} - \frac{3}{2}A_0\omega_x^2, \\
\ddot{A}_1 &= \frac{10\dot{A}_0}{3A_0}\dot{A}_1 + \left(-\frac{3}{2}\omega_x^2 + 9g_{1\mathrm{d}}A_0^2 - \frac{5\dot{A}_0^2}{3A_0^2}\right)A_1 \\
&\quad +\varepsilon(t), \quad (8) \\
\varepsilon(t) &= 3V_1\cos\omega t A_0 - \frac{4}{3}\gamma\dot{A}_0. \quad (9)
\end{aligned}$$

The leading order equation has the homoclinic solution[12]

$$A_0 = \frac{\omega_x}{2}\sqrt{\frac{-1}{g_{1\mathrm{d}}}}\mathrm{sech}\left[\frac{3}{2}\omega_x(t-t_0)\right], \quad (10)$$

where t_0 is the initial time. Applying our perturbation technique to Eq. (8), we immediately write down its general solution in the integral form as[24]

$$\begin{aligned}
A_1 &= A_1''\int_{C_1}^{t} A_0^{10/3}\varepsilon(t)A_1'\,\mathrm{d}t \\
&\quad -A_1'\int_{C_2}^{t} A_0^{10/3}\varepsilon(t)A_1''\,\mathrm{d}t. \quad (11)
\end{aligned}$$

Here C_1 and C_2 are arbitrary integral constants which depend on initial conditions. A_1' and A_1'' are the two fundamental solutions of Eq. (8) at $\varepsilon(t) = 0$, which are easily derived as

$$\begin{aligned}
A_1' &= \dot{A}_0 \\
&= -\frac{3}{4}\omega_x^2\sqrt{-\frac{1}{g_{1\mathrm{d}}}}\mathrm{sech}\left[\frac{3}{2}\omega_x(t-t_0)\right] \\
&\quad \times\tanh\left[\frac{3}{2}\omega_x(t-t_0)\right], \quad (12) \\
A_1'' &= \dot{A}_0\int A_0^{10/3}\dot{A}_0^{-2}\,\mathrm{d}t. \quad (13)
\end{aligned}$$

Given the form of $A(t)$, from Eq. (4) we obtain

$$\begin{aligned}
B &= B(t_0)\left[\frac{A\,\mathrm{e}^{2\gamma(t-t_0)}}{A(t_0)}\right]^{1/3}, \\
b &= \frac{\gamma}{3} - \frac{\dot{A}}{3A}, \\
a &= -g_{1\mathrm{d}}\int B^2(t_0)\left[\frac{A\,\mathrm{e}^{2\gamma(t-t_0)}}{A(t_0)}\right]^{2/3}\mathrm{d}t \quad (14)
\end{aligned}$$

with $A(t_0)$ and t_0 being arbitrary constants adjusted by the initial conditions. Inserting Eqs. (10) and (11) into Eq. (6), we have the form of function $A(t)$. From Eq. (14) we can give the explicit forms of functions $B(t)$, $a(t)$ and $b(t)$. Combining these functions with Eqs. (3) and (5), we can easily obtain the corresponding explicit forms of the formally exact solution, atomic density and flow velocity.

According to Eqs. (12) and (13), we see that the chaotic perturbed solution Eq. (11) is unbounded generally, because of the unboundedness of function A_1'' at $t \to \infty$. It implies that the system is unstable. However, we can prove by using l'Hospital rule that the perturbed solution is bounded if and only if the conditions

$$I_{\pm} = \lim_{t\to\pm\infty}\int_{C_1}^{t} A_0^{10/3}\varepsilon(t)A_1'\,\mathrm{d}t = 0 \quad (15)$$

are satisfied. It is worth while noting that the boundedness conditions (15) contain the Melnikov's chaos criterion $M(t_0) = I_+ - I_- = 0$, which measures the distance between stable and unstable manifolds in the Poincaré sections. The simple zero of the Menikov function indicates the existence of Smale-horseshoe chaos.[29] Under conditions (15) we call Eq. (11) the chaotic solution. Such a solution is analytically bounded but numerically unbounded, because of the uncomputability of the chaotic solution.

Inserting Eqs. (9), (10) and (12) into the Melnikov's chaos criterion $M(t_0) = I_+ - I_- = 0$, we obtain

$$\begin{aligned}
M(t_0) &= 3V_1\sin\omega t_0 D_1\left(\frac{\omega_x}{2}\right)^{16/3}\left(\frac{-1}{g_{1\mathrm{d}}}\right)^{8/3} - 4\gamma D_2\left(\frac{\omega_x}{2}\right)^{19/3}\left(\frac{-1}{g_{1\mathrm{d}}}\right)^{8/3} = 0, \\
D_1 &= \int_{-\infty}^{\infty}\sin\left(\frac{2\omega\xi}{3\omega_x}\right)(\mathrm{sech}\,\xi)^{16/3}\tanh\xi\,\mathrm{d}\xi, \quad D_2 = \int_{-\infty}^{\infty}(\mathrm{sech}\,\xi)^{16/3}(\tanh\xi)^2\,\mathrm{d}\xi \quad (16)
\end{aligned}$$

with $\xi = 3\omega_x(t - t_0)/2$. From Eq. (16) we have the chaotic region

$$V_1 \geq \frac{2D_2\gamma\omega_x}{3D_1} \tag{17}$$

in parameter space, where $D_1 = D_1(\omega_x, \omega)$ is a function of ω_x and ω, D_2 is independent of them. Generally speaking, equation (17) is a necessary condition for the onset of chaos. For a set of fixed parameters, equation (17) gives a threshold value of driving strength. The system may undergo an evolution from regular motion to chaotic motion when the driving strength exceeds the threshold value.

For the sake of seeing clearly the dependence of chaotic region on system parameters, from Eq. (17) we plot driving strength V_1 versus driving frequency ω in Fig. 1, where the dash curve represents the case where $\omega_x = 0.6$ and $\gamma = 0.2$, and the solid curve refers to the case where ω_x is the same and feeding strength is smaller, i.e., $\omega_x = 0.6$ and $\gamma = 0.02$. The adjustment of feeding strength can be performed roughly by changing the atomic number of the thermal cloud or its temperature. In Fig. 1, the areas above the curves correspond to Melnikov chaotic regions in which the evolution of the atomic number density may possess the properties of Smale-horseshoe chaos; those below the curves denote the regions of regular motion, where chaos cannot exist. When $\gamma = 0.02$ is given, region E is a regular region and regions F and G are both chaotic regions. For $\gamma = 0.2$, regular regions are enlarged to regions E and F and the chaotic region is reduced to region G. Therefore, the enhancement of feeding strength will reduce the chaotic regions. That is to say, the increase of feeding strength can suppress the chaos.

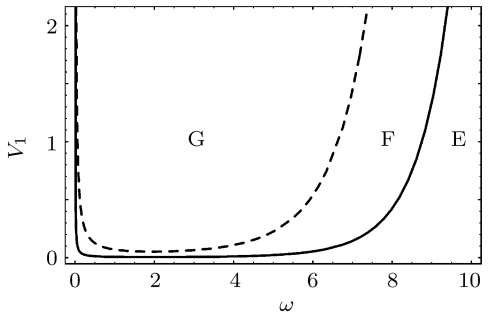


Fig. 1. Plots of driving strength V_1 versus driving frequency ω, showing the chaotic regions in parameter space with parameters being (a) $\omega_x = 0.6$ and $\gamma = 0.2$ (dash curve), and (b) $\omega_x = 0.6$ and $\gamma = 0.02$ (solid curve). V_1 and ω are in units of $m\omega_0^2$ and ω_0, respectively. ω_x is in the same units as ω.

Given the chaotic regions, we can let the system stay in a chaotic state or not, by adjusting the driving strength V_1 or driving frequency ω. For example, from Fig. 1, we easily see that the system can leave chaotic regions by reducing the driving strength V_1 to a small value for a fixed value of ω or by increasing the driving frequency ω to a high value for a fixed value of V_1. As shown in Fig. 1, the bigger the value of V_1 we take, the bigger the value of ω we need for making the system enter into chaotic regions. Meanwhile, according to Eq. (17) we see that the threshold value of driving strength is proportional to feeding strength. When the feeding strength is very weak, the critical value of V_1 is small, but a strong feeding strength will lead to a higher critical V_1.

3. Numerical simulations of chaotic and regular motions

The chaotic region of Eq. (17) is given based on a weak driving strength and small feeding strength. For a strong driving strength and big feeding strength which cannot be treated as perturbations, the Melnikov function method is not effective, then a numerical analysis for the system is needed.

In order to explore the analytically insolvable Eq. (6), we solve it numerically by using the software package MATHEMATICA.[12] We fix $\omega_x = 0.6$, $g_{1\mathrm{d}} = -0.375$, $\omega = 6$ and take stochastic initial conditions $\{A(0) \in [-1.5, 1.5],\ \dot{A}(0) \in [-1.5, 1.5]\}$ to plot three groups of Poincaré sections in the equivalent phase space $(A, \dot{A})$ of chaotic regions and regular regions as shown in Fig. 2. Here any Poincaré section is a discrete set of phase space points in each period of the external potential. Each group contains 20 Poincaré sections. In Figs. 2(a) and 2(b), we show the superpositions of 20 Poincaré sections in chaotic regions for driving strength $V_1 = 4$, feeding strength (a) $\gamma = 0.01$ and (b) $\gamma = 0.1$, respectively. Figure 2(c) presents the superpositions of 20 Poincaré sections in regular regions for $\gamma = 0.2$ and $V_1 = 0.5$. Comparing Fig. 2(a) with Fig. 2(b), we find that the phase space points gradually reduce with the increase of feeding strength. There are chaotic orbits as well as regular orbits in chaotic regions. From Fig. 2(c), we see that the Poincaré section is composed of several points which denote regular orbits. Thus, in regular regions there are no chaotic orbits except regular orbits.

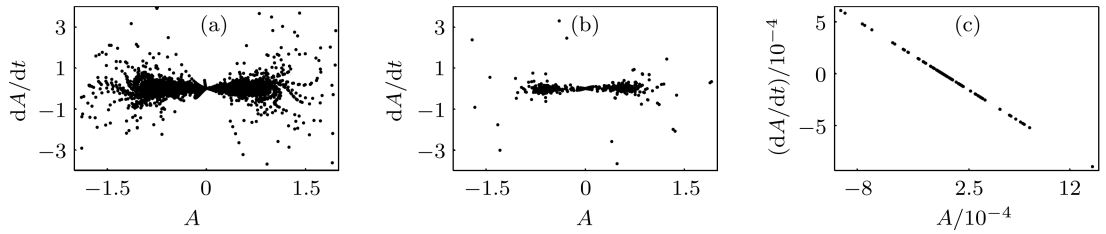


Fig. 2. Poincaré sections in dimensionless phase space $(A, \dot{A})$ for parameters $\omega_x = 0.6$, $g_{1d} = -0.375$, $\omega = 6$ and (a) $V_1 = 4$, $\gamma = 0.01$; (b) $V_1 = 4$, $\gamma = 0.1$; (c) $V_1 = 0.5$, $\gamma = 0.2$. Panels 2(a) and 2(b) correspond to chaotic regions. Panel 2(c) corresponds to regular regions. Three panels each with 20 Poincaré sections, are for different initial conditions.

In regular regions, the small change of bound conditions or system parameters will bring a small correction to the system state which can be ignored in a good approximation. So, there will be little influence on the phase space orbits if we change initial conditions or system parameters. However, in chaotic regions, the small change of initial conditions or system parameters may lead to a transition from regular state to chaotic state or reverse, which cannot be ignored. So we will discuss the effects of system parameters on phase space orbits in chaotic regions.

Starting from Eq. (6), we select two sets of initial conditions to plot the phase space orbits of the Poincaré section in chaotic regions as presented in Fig. 3, where $V_1 = 6.45$, $\gamma = 0.02$, $\omega_x = 0.6$, $g_{1d} = -0.375$, $\omega = 6$ and for (a) $A(0) = -0.1$, $\dot{A}(0) = 1.4$; (b) $A(0) = 0.6$, $\dot{A}(0) = -0.02$. In Fig. 3(a), for the initial data $A(0) = -0.1$ and $\dot{A}(0) = 1.4$, there are only several points on the Poincaré section which denote regular orbits. When the initial data are changed into $A(0) = 0.6$ and $\dot{A}(0) = -0.02$, some confused points which mean chaotic orbits appear in the region near the centre of phase space as shown in Fig. 3(b). This transition from regular state to chaos is caused by the small change in initial condition. So chaos sensitively depends on initial condition in chaotic regions.

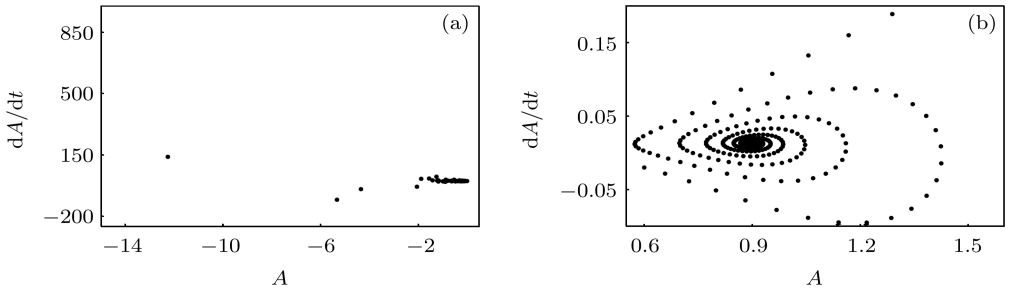


Fig. 3. Poincaré sections in dimensionless phase space $(A, \dot{A})$ for parameters $V_1 = 6.45$, $\gamma = 0.02$, $\omega_x = 0.6$, $g_{1d} = -0.375$, $\omega = 6$ and the initial conditions (a) $A(0) = -0.1$, $\dot{A}(0) = 1.4$ and (b) $A(0) = 0.6$, $\dot{A}(0) = -0.02$.

Now we investigate the phase space orbits in chaotic regions for fixed initial conditions with different feeding strengths. We plot the phase space orbits on the Poincaré sections in Fig. 4 for (a) $\gamma = 0.002$, (b) $\gamma = 0.2$, where other parameters are the same as those in Fig. 3, the driving strength is taken as $V_1 = 3.8$ and the initial data are set as $A(0) = 50\sqrt{3}$ and $\dot{A}(0) = -50$.

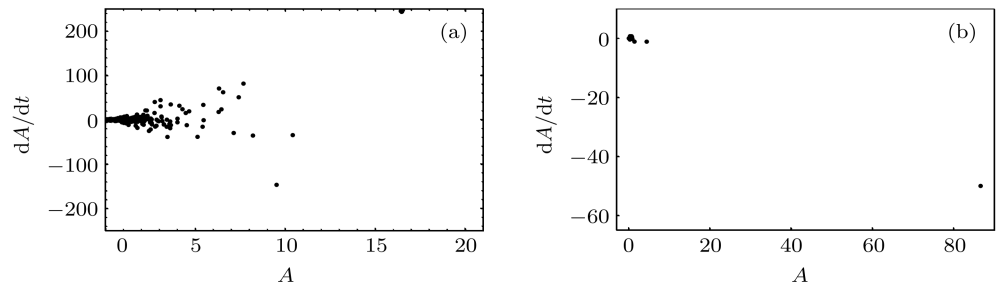


Fig. 4. Poincaré sections in dimensionless phase space $(A, \dot{A})$ for parameters $V_1 = 3.8$, initial conditions $A(0) = 50\sqrt{3}$, $\dot{A}(0) = -50$ and (a) $\gamma = 0.002$, (b) $\gamma = 0.2$. The other parameters are the same as those in Fig. 3.

From Fig. 4(a) we see that for $\gamma = 0.002$, the phase space orbits are chaotic. With the increase of feeding strength, the phase space orbits gradually become regular. When the feeding strength reaches 0.2, there are several points in the phase space which refer to regular orbits. The phase space orbits transform from chaotic motion to regular motion, which means that the change of feeding strength has a suppressive effect on chaos. Therefore we can control such a system of BEC to a chaotic or regular state by adjusting the feeding strength. This method can also be extended to other physical systems.

4. Effects of feeding strength on the number of condensed atoms

We discuss the effects of various feeding strengths on the number of condensed atoms. We consider two cases: one is the boundary values fixed at $\pm L$ and the other is the free boundary with the shock fronts $\pm x_0$ varying with time.

The considered BEC is created initially in a range near the potential centre. The number of condensed atoms $N(t)$ varies with time because of the feeding from the nonequilibrium thermal cloud. At any time, the number of condensed atoms is expressed as

$$\begin{aligned} N(t) &= \int_{-x_0}^{x_0} |\psi(x,t)|^2 \mathrm{d}x \\ &= \frac{2}{3}A^2(t)x_0^3 + 2B^2(t)x_0. \end{aligned} \tag{18}$$

At the initial time $t_0 = 0$, the boundary atomic density is $\rho(0) = \rho_0 = A^2(0)L^2 + B^2(0)$ and the number of condensed atoms is $N(0) = 2A^2(0)L^3/3 + 2B^2(0)L = 2\rho_0 L - 4A^2(0)L^3/3$. We will take $L = 1$, $\rho_0 = 10^4$ and $N(0) = 10^4$ in the following. According to these data, we gain $A(0) = 50\sqrt{3}$ and $B(0) = 50$. Here, L and ρ_0 are in units of l_0 and $1/l_0$, respectively.

First we discuss the case of "nonpropagated" shock wave with a fixed boundary. All atoms are confined between the boundary $x = \pm L$. Combining Eq. (14) with Eq. (18), we obtain the number of condensed atoms as

$$\begin{aligned} & N(t) \\ &= \int_{-L}^{L} [A^2(t)x^2 + B^2(t)] \mathrm{d}x \\ &= \frac{2}{3}A^2(t)L^3 + \frac{2B^2(0)A^{2/3}(t)\,\mathrm{e}^{4\gamma t/3}L}{A^{2/3}(0)}, \end{aligned} \tag{19}$$

where L, $A(0)$ and $B(0)$ are predetermined constants. From Eqs. (19) and (6), by taking the constants $L = 1$, $A(0) = 50\sqrt{3}$, $B(0) = 50$, with the other parameters being the same as those of Fig. 4, we numerically plot the time evolutions of the number of condensed atoms in Fig. 5 for (a) $\gamma = 0.002$, (b) $\gamma = 0.2$ in the case of fixed boundary. As we see in Fig. 5(a), for $\gamma = 0.002$, the number of condensed atoms alternately collapses and revives, and may increase over the initial atomic number at a certain time. When the feeding strength increases to 0.2, the number of condensed atoms is enlarged rapidly compared with that of Fig. 5(a) as shown in Fig. 5(b). From the inset in Fig. 5(b) we see that the number of condensed atoms aperiodically oscillates in time at the beginning of a period. So for the case of "nonpropagated" shock wave with fixed boundary, the number of condensed atoms rises quickly with the increase of feeding strength.

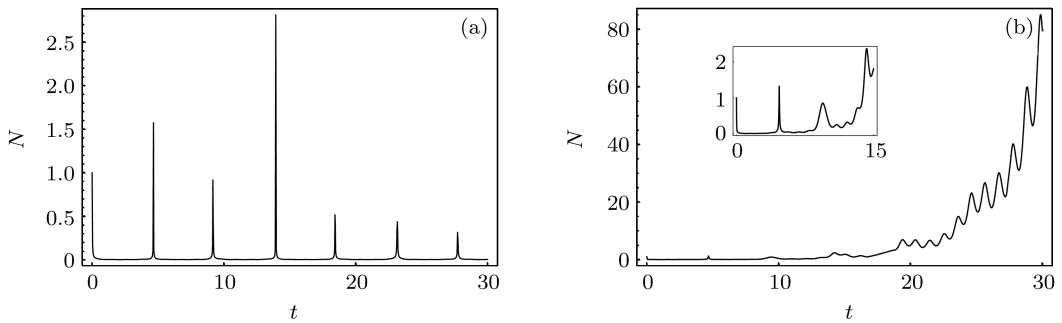


Fig. 5. Time evolutions of the number of condensed atoms for the case of fixed boundary for constants $L = 1$, $A(0) = 50\sqrt{3}$, $B(0) = 50$ and (a) $\gamma = 0.002$, (b) $\gamma = 0.2$. The other parameters are the same as those of Fig. 4. The inset in panel (b) describes the time evolution of the number of condensed atoms from $t = 0$ to $t = 15$. The number of condensed atoms N is normalized in units of 10^4 and t in units of ω_0^{-1}.

Then we study a kind of metastable shock wave, where the constant atomic density $\rho(x_0) = \rho_0$ is kept at

the front position $x_0(t)$ for a free boundary at any time. Combining Eq. (5) with Eq. (14), we have the constant atomic density of the shock front, $\rho_0 = A^2(t)x_0^2(t) + B^2(t)$, so the shock front position $x_0(t)$ reads

$$x_0(t) = \pm\left[\frac{\rho_0}{A^2(t)} - \frac{B^2(t)}{A^2(t)}\right]^{1/2} = \pm\left[\frac{\rho_0}{A^2(t)} - \frac{B^2(0)\,\mathrm{e}^{4\gamma t/3}}{A^{2/3}(0)A^{4/3}(t)}\right]^{1/2}. \tag{20}$$

The constants will be taken as $\rho_0 = 10^4$, $A(0) = 50\sqrt{3}$ and $B(0) = 50$ in calculations. The $A(t)$ in Eq. (20) is time-dependent, with phase orbits being chaotic or regular, so the shock wave front $x_0(t)$ may periodically or chaotically oscillate. The time evolution of the number of condensed atoms is written as

$$N(t) = \int_{-x_0}^{x_0} [A^2(t)x^2 + B^2(t)]\,\mathrm{d}x = \frac{2}{3}A^2(t)x_0^3(t) + \frac{2B^2(0)A^{2/3}(t)\,\mathrm{e}^{4\gamma t/3}x_0(t)}{A^{2/3}(0)}. \tag{21}$$

Combining Eq. (6) with Eqs. (20) and (21), we plot the time evolutions of the number of condensed atoms and shock front position for the case of free boundary as shown in Fig. 6, by using the same parameters as those in Fig. 5, $\rho_0 = 10^4$ and for $\gamma = 0.002$ in Figs. 6(a) and 6(b), and $\gamma = 0.2$ in Figs. 6(c) and 6(d). We plot only the positive $x_0(t)$, since the negative $x_0(t)$ can be seen through spatial symmetry of the system. From Fig. 6(a) with $\gamma = 0.002$, we find that the number of condensed atoms and the shock front position aperiodically oscillate with approximate constant amplitudes, which indicates the metastability of the system. However, when the feeding strength reaches 0.2, the front position and the atomic number oscillate aperiodically with decaying amplitudes, which means the loss of the metastability in the strong feeding case.

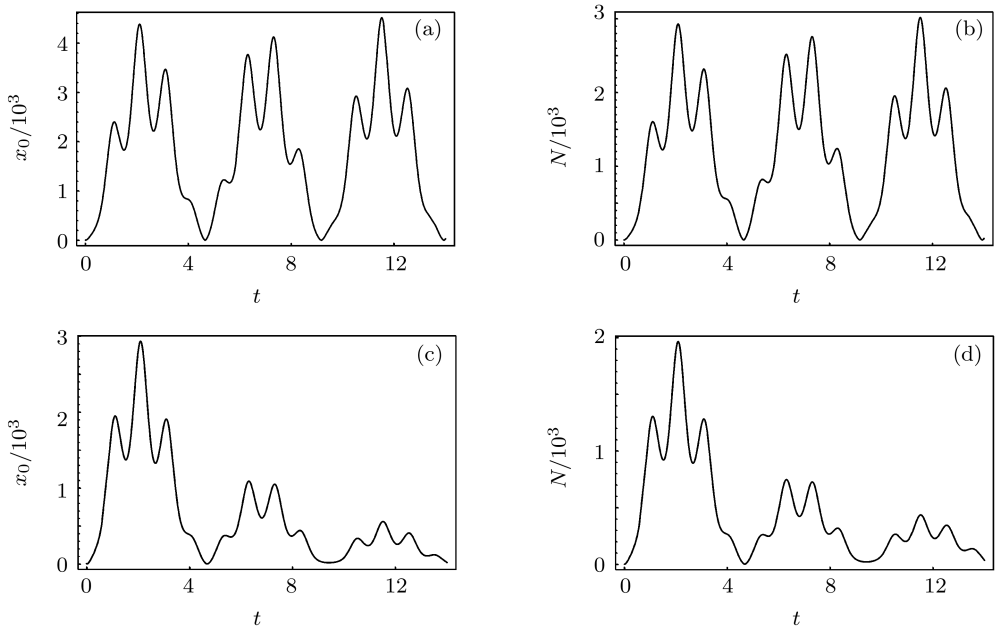


Fig. 6. Time evolutions of atomic number and front position for the case of free boundary with $\rho_0 = 10^4$ and $\gamma = 0.002$ (a), (b), $\gamma = 0.2$ (c), (d). The other parameters are the same as those of Fig. 5. The same units as those in Fig. 5 are adopted.

5. Conclusions and discussion

We have studied a 1D open BEC system driven by a time-periodic inverted-harmonic potential, considering the feeding effect. When the driving strength and the feeding strength are both very weak, using the Melnikov function to predict the onset of chaos is a valid analytical technique. A formally exact solution of the time-dependent GPE is set up. We obtained the chaotic perturbed solution by employing the direct perturbation method. The chaotic regions are gained by using the Melnikov function method. When the driving strength and the feeding strength are strong enough, we cannot treat them as perturbations to the system, then a numerical approach is necessary.

Through simulating numerically, we investigated

the phase space orbits and the time evolutions of the number of condensed atoms with different system parameters. We found that the chaotic regions can be enlarged by reducing the feeding strength. The numerical results also indicate that the increase of feeding strength plays a role in suppressing the chaos. For the case of "nonpropagated" shock wave with fixed boundary, the number of condensed atoms rises rapidly with the increase of feeding strength. For the free boundary case, we investigated a kind of metastable shock wave with the front density being unchanged, and found that a stronger feeding strength can cause the loss of the metastability of the system. The feeding strength can be adjusted roughly by changing atomic number of the thermal cloud. It is well known that chaos can emerge in the process of BECs collapsing[34] and may play a destructive role in the BEC systems. Therefore predicting and controlling chaos are quite important for the creation and the application of BECs. Our analytical and numerical results have supplied a qualitative method of controlling the regular and chaotic states through adjusting the system parameters, which may be useful.

References

[1] Whitham G B 1999 *Linear and Nonlinear Waves* (New York: Wiley)

[2] Courant R and Friedrichs K O 1948 *Supersonic Flow and Shock Waves* (Berlin: Springer-Verla)

[3] Shugaev F V and Shtemenko L S 1998 *Propagation and Reflection of Shock Waves* (Singapore: World Scientific)

[4] Gurovich V T, Grinenko A and Krasik Y E 2007 *Phys. Rev. Lett.* **99** 124503

[5] Shvartsburg A B, Stenflo L and Shukla P K 2002 *Euro. Phys. J.* B **28** 71

[6] Brazhnyi V A, Kamchatnov A M and Konotop V V 2003 *Phys. Rev.* A **68** 035603

[7] Kulikov I and Zak M 2003 *Phys. Rev.* A **67** 063605

[8] Damski B 2004 *Phys. Rev.* A **69** 043610

[9] Dutton Z, Budde M, Slowe C and Hau L V 2001 *Science* **293** 663

[10] Simula T P, Engels P, Coddington I, Schweikhardand V C, Cornell E A and Ballagh R J 2005 *Phys. Rev. Lett.* **94** 080404

[11] Peréz-García V M, Konotop V V and Brazhnyi V A 2004 *Phys. Rev. Lett.* **92** 220403

[12] Hai W H, Zhu Q Q and Rong S G 2009 *Phys. Rev.* A **79** 023603

[13] Castin Y and Dum R 1996 *Phys. Rev. Lett.* **77** 5315

[14] Xu Z J, Shi J Q, Li Z and Cai P G 2006 *Acta Phys. Sin.* **55** 5366 (in Chinese)

[15] Liang Z X, Zhang Z D and Liu W M 2005 *Phys. Rev. Lett.* **94** 050402

[16] Abdullaev F Kh and Galimzyanov R 2003 *J. Phys.* B **36** 1099

[17] Chong G S and Hai W H 2007 *J. Phys.* B **40** 211

[18] Zhou Z, Yu H Y and Yan J R 2010 *Chin. Phys.* B **19** 010304

[19] Sackett C A, Stoof H T C and Hulet R G 1998 *Phys. Rev. Lett.* **80** 2031

[20] Kagan Y, Muryshev A E and Shlyapnikov G V 1998 *Phys. Rev. Lett.* **81** 933

[21] Gammal A, Frederico T, Tomio L and Chomaz P 2000 *Phys. Rev.* A **61** 051602 (R)

[22] Li Y and Hai W H 2005 *J. Phys.* A **38** 4105

[23] Mu A X, Zhou X Y and Xue J K 2008 *Chin. Phys.* B **17** 764

[24] Hai W H, Zhang X L, Huang W L and Chong G S 2001 *Int. J. Bifur. Chaos* **11** 2263

[25] Huang G X 2004 *Chin. Phys.* **13** 1866

[26] Hai W H, Duan Y W and Pan L X 1997 *Phys. Lett.* A **234** 198

[27] Hai W H, Rong S G and Zhu Q Q 2008 *Phys. Rev.* E **78** 066214

[28] Fang J S 2008 *Chin. Phys.* B **17** 3996

[29] Melnikov V K 1963 *Trans. Mosc. Math. Soc.* **12** 1

[30] Zhu Q Q, Hai W H and Rong S G 2009 *Phys. Rev.* E **80** 016203

[31] Xu J, Hai W H and Li H 2007 *Chin. Phys.* **16** 2244

[32] Parthasarathy S 1992 *Phys. Rev.* A **46** 2147

[33] Hoefer M A, Ablowitz M J, Coddington I, Cornell E A, Engels P and Schweikhard V 2006 *Phys. Rev.* A **74** 023623

[34] Saito H and Ueda M 2001 *Phys. Rev. Lett.* **86** 1406